Journal of Sound and Vibration (1997) **206**(1), 39–60

SUBHARMONIC OSCILLATIONS IN HARMONICALLY EXCITED MECHANICAL SYSTEMS WITH CYCLIC SYMMETRY

S. Samaranayake

Department of Mathematics and Computer Science, University of Wisconsin-Whitewater, Whitewater, WI 53190, *U.S.A.*

AND

A. K. Bajaj

School of Mechanical Engineering, Purdue University, West Lafayette, IN 47907, *U.S.A.*

(*Received* 9 *August* 1996, *and in final form* 9 *April* 1997)

The third-order subharmonic oscillations in weakly non-linear cyclic symmetric structures with multiple degrees of freedom are studied. These strongly coupled cyclic structures, in their linear approximation, are known to possess pairwise double-degenerate natural frequencies with orthogonal normal modes. The asymptotic method of averaging is used to study the nonlinear interactions between the pairs of modes with nearly identical natural frequencies when the external excitation is nearly three times the natural frequency of the modes being excited. A careful local bifurcation analysis of the averaged equations is conducted to study the effects of frequency mistuning and excitation amplitudes, as well as the modal damping in the system. Subharmonic standing and traveling wave type solutions, Hopf bifurcation from traveling wave solutions to quasiperiodic responses, period-doubling bifurcations, and Silnikov type chaos are found to exist in the averaged system.

1. INTRODUCTION

Structural systems are in general complex, and often consist of a large number of substructures acting as a single entity. An important class of structural systems found in engineering applications are those with cyclic symmetry, which are composed of nominally identical substructures. They arise naturally, among others, in large circular space antennas, bladed disk assemblies, and magnetic storage devices. The cyclic symmetry of the structure implies that most of the frequencies for the linear model appear in pairwise double-degenerate pairs with distinct orthonormal normal modes. Because of manufacturing errors and engineering tolerances, these structures inevitably involve minor deviations from the idealized structural models. Under appropriate conditions, these perturbations from symmetric structures may result in unexpected behavior in the response of the linear system [1]. More typically, the non-linear response of these cyclic structures to harmonic excitations is quite complex, and is a result of natural modal interactions that arise due to the 1:1 internal resonance in the linear modes of vibrations of the system [2, 3].

One of the important characteristics of the response of non-linear systems is the existence of subharmonic and superharmonic resonances. In some regions of the parameter space, non-linear systems may possess a response with a frequency which is a multiple of the

0022–460X/97/360039 + 22 $25.00/0/sv971075

excitation frequency. In general, these responses coexist with a response at the excitation frequency, and initial conditions determine which of the steady-state responses is achieved. Mook *et al*. [4] investigated the subharmonic response of structural elements, such as beams, arches, plates, and shells, to a harmonic excitation, in the presence as well as absence of internal resonance. In the presence of a 2:1 internal resonance, it was noted that energy may be transferred between the two modes. Also, internal resonance causes a saturation phenomenon and a role reversal between the directly and the indirectly excited modes. Shyu *et al*. [5] investigated subharmonic and superharmonic resonances in a slender, elastic, cantilevered beam with equal principal moments of inertia, subjected to a transverse constant and harmonic load. The effects of non-linear curvature, non-linear inertia, viscous damping, and static load were examined. Cubic terms in the governing equations lead to subharmonic and superharmonic resonances of third order. The inclusion of static load produced quadratic terms in the governing equations, and hence subharmonic and superharmonic resonances of second order were also present for the system. Steady state whirling motions were found to be possible in all these cases of secondary resonances. Vakakis [6] examined fundamental and subharmonic resonances in a two-degree-of-freedom oscillator system with cubic non-linearities and linear viscous damping. Nayfeh and Vakakis [7] examined subharmonic responses in thin, geometrically non-linear, circular plates. Two types of forced subharmonic responses were detected, namely, subharmonic standing waves and traveling waves. Quasiperiodic motions via a Hopf bifurcation were also detected.

In the present work, a model of a multi-degree-of-freedom cyclic system is studied for its third order subharmonic resonance. This model was examined for its response under primary resonance in the work of Samaranayake *et al*. [3]. The system possesses cubic non-linearities, and the method of averaging is used to derive the amplitude or the averaged equations. A careful computer-assisted local bifurcation analysis for steady state constant solutions of the averaged equations is performed. Using a two mode approximation, the original equations of motion are directly integrated to show the validity of the method of averaging in predicting the existence of amplitude-modulated solutions.

2. EQUATIONS OF MOTION AND AVERAGED EQUATIONS

As many of the previous studies have indicated, all cyclic structures with monocoupled substructures ultimately can be reduced to the same form of the governing non-linear equations of motions. Consequently, the response of every finite degree-of-freedom system of this type can be captured by a simple model in which the individual subsystem is a one-degree-of-freedom system with a non-linear stiffness element. Thus, a cyclic system consisting of n identical particles of mass m each, arranged in a ring, and interconnected by non-linear extensional springs is considered, and that all the masses are assumed to be hinged to the ground by non-linear torsional springs (see Figure 1) [3]. Since the details are well documented in reference [3], only the modelling assumptions and the equations of motion are summarized.

Let x_i be the tangential displacement of the ith particle. Then,

$$f_{ij} = k_1(x_i - x_j) + \epsilon k_2(x_i - x_j)^3 \tag{1}$$

is the force in the spring between the ith particle and its jth neighboring particle, and

$$f_{it} = T_1 x_i/a^2 + \epsilon T_2 x_i^3/a^4 \tag{2}$$

is the force induced on the ith mass particle due to the torsional spring attached to it. The particle motions are viscously damped with $\epsilon\, \mathrm{d}\dot{x}_i$ as the damping force. The parameter ϵ

is small, $0 \leqslant \epsilon \ll 1$, and reflects the smallness of the damping and the non-linearity coefficients.

The equation of motion for the ith mass particle in the cyclic structure can then be written in the form:

$$m\ddot{x}_i + (T_1/a^2 + 2k_1)x_i - k_1(x_{i-1} + x_{i+1}) + \epsilon f_i = F_i^{ex}(t), \tag{3}$$

where

$$f_i = k_2\{(x_i - x_{i+1})^3 + (x_i - x_{i-1})^3\} + T_2 x_i^3/a^4 + \mathrm{d}\dot{x}_i, \tag{4}$$

and where $F_i^{ex}(t)$ is an external force on the ith particle.

Thus, there are two non-linear stiffness terms, one arising from the individual torsional stiffness, and the other arising from the coupling between the neighboring particles. A new time scale $\tau = \bar{\omega}t$ is defined, where $\bar{\omega} = \{T_1/ma^2\}^{1/2}$. The equations of motion for the n-degree-of-freedom cyclic structure can then be written in a matrix form as

$$[\mathbf{x}''] + [\mathbf{K}][\mathbf{x}] + (\epsilon/m\bar{\omega}^2)[\mathbf{F}] = [\mathbf{F}^{ex}]/m\bar{\omega}^2, \tag{5}$$

where

$$[\mathbf{K}] = \begin{bmatrix} 1+2k & -k & 0 & \cdots & \cdot & -k \\ -k & 1+2k & 0 & \cdots & \cdot & \cdot \\ 0 & \cdot & \cdot & \cdots & \cdot & \cdot \\ \cdot & \cdot & \cdot & \cdots & \cdot & -k \\ -k & 0 & \cdot & \cdots & -k & 1+2k \end{bmatrix}, \tag{6}$$

and $[\mathbf{F}] = [f_1\ f_2\ \cdots\ f_n]^{\mathrm{T}}$.

Note that this model can be considered as a first approximation of a bladed disk or an antenna-type structure consisting of identical beams that are clamped to a rigid base and are coupled by non-linear stiffness elements. When the beam deflections are modelled by their pth linear flexural modes, a one-mode Galerkin analysis leads to a system similar to equations (5) (reference [1]).

One wishes to study the response of the system of equations (5) when the parameter ϵ is small. The linear system (when $\epsilon = 0$) has mostly pairwise degenerate natural frequencies

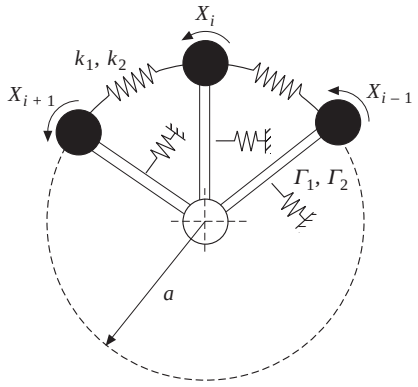

Figure 1. The non-linear cyclic system.

with orthogonal normal modes. One possible set of mode shapes of the n-degree-of-freedom cyclic system is as follows [1, 2]:

$$[\mathbf{U}_0] = [1 \quad 1 \quad 1 \quad \cdots \quad 1]^{\mathrm{T}},$$
$$[\mathbf{U}_j^c] = [\cos\alpha_j \quad \cos 2\alpha_j \quad \cdots \quad \cos n\alpha_j]^{\mathrm{T}},$$
$$[\mathbf{U}_j^s] = [\sin\alpha_j \quad \sin 2\alpha_j \quad \cdots \quad \sin n\alpha_j]^{\mathrm{T}}, \tag{7}$$

where $\alpha_j = 2\pi j/n$; $j \in [1, (n-1)/2]$ for n odd and $j \in [1, (n-2)/2]$ for n even, and

$$[\mathbf{U}_{n/2}] = [\cos\pi \quad \cos 2\pi \quad \cdots \quad \cos n\pi]^{\mathrm{T}} \tag{8}$$

only for n even. The modes $[\mathbf{U}_j^c]$ and $[\mathbf{U}_j^s]$ are, respectively, the "cos $-$ j" and "sin $-$ j" modes, and correspond to the same natural frequency ω_j. The linear natural frequencies of the cyclic structure are given by

$$\omega_j = 1 + 2k\{1 - \cos\alpha_j\}, \begin{cases} j = 0, 1, 2, \quad \cdots (n-1)/2 & \text{for } n \text{ odd}, \\ j = 0, 1, 2, \quad \cdots n/2 & \text{for } n \text{ even}. \end{cases} \tag{9}$$

Most of these natural frequencies appear as double eigenvalues so long as the coupling stiffness k_1 is not small (or weak). In the case of weak coupling all the n natural frequencies are clustered in a small neighborhood of the natural frequency of the individual subsystem.

In the above discussion, the system has been assumed to be cyclic. This is only an idealization and there are inevitable symmetry-breaking perturbations present in any realistic structure. These perturbations destroy the double degeneracy of eigenvalues ω_j, and the corresponding eigenfunctions are also perturbed from the "cos $-$ j" and "sin $-$ j" eigenfunctions. For systems dependent on only a single small parameter, it is well known from perturbation theory for symmetric systems [8] that, for a generic perturbation, every double eigenvalue splits into two distinct eigenvalues. These eigenvalues and the corresponding distinct eigenvectors, which are also a perturbation of the "cos $-$ j" and "sin $-$ j" eigenvectors, can be obtained as a power series in the small perturbation parameter. Let ω_{jc} and ω_{js} be the two eigenvalues with $\omega_{jc} \to \omega_j$ and $\omega_{js} \to \omega_j$ as the symmetry-breaking perturbation goes to zero. In the analysis to follow, one allows for the system to be mistuned or perturbed from cyclicity. Thus, the small difference in the two frequencies, $\omega_{jc} - \omega_{js}$, represents internal mistuning in the structure.

In order to study non-linear interactions between the pairs of modes with identical (or nearly identical) linear natural frequencies, and to study the subharmonic response of the cyclic system, one assumes that the external harmonic excitation $[\mathbf{F}^{ex}](t)$ is of $O(1)$ in ϵ, and is given by

$$[\mathbf{F}^{ex}] = f_0[\mathbf{\Gamma}] \cos\bar{\Omega}t = f_0[\mathbf{\Gamma}] \cos\Omega\tau \quad \text{and} \quad \bar{\Omega} = \bar{\omega}\Omega. \tag{10}$$

One now utilizes the method of averaging [9, 10] to study the dynamics of the weakly non-linear, non-autonomous system defined by equations (5). It transforms the equations of motion to an autonomous set of first order ordinary differential equations which is referred to as the averaged equations. These averaged equations represent the slow-time evolution of the amplitudes and phases of subharmonic motion of the interacting linear modes in resonance.

Depending on the type of external excitation and the relationship of the frequency with the system linear frequencies, primary, secondary, and combination resonances may arise in the dynamics of the strongly coupled system. In order to study the third order subharmonic resonance, the excitation frequency Ω is assumed to be nearly three times the

degenerate natural frequency ω_j. The external excitation is assumed to be spatially distributed like one of the corresponding two modes in resonance and is orthogonal to the other mode, that is,

$$[\mathbf{F}^{ex}] = (f_0/e)\,[\mathbf{U}_j^c]\cos\bar{\Omega}t.$$

The only modes that can be excited by this type of forcing and contribute to the response at the lowest order of approximation are the "cos $-\,j$" and "sin $-\,j$" modes. Hence, the steady state subharmonic response of the system in equations (5) can be expressed in the form

$$[\mathbf{x}] = \frac{1}{e}\left\{B_j(\tau)[\mathbf{U}_j^c]\cos\left(\frac{\Omega\tau}{3}+\beta_j(\tau)\right) + C_j(\tau)[\mathbf{U}_j^s]\cos\left(\frac{\Omega\tau}{3}+\gamma_j(\tau)\right) + \sigma[\mathbf{U}_j^c]\cos\Omega\tau\right\}, \quad (11)$$

where

$$e = \left\{\sum_{i=1}^{n}\cos^2 i\alpha_j\right\}^{1/2} = \left\{\sum_{i=1}^{n}\sin^2 i\alpha_j\right\}^{1/2} = \sqrt{n/2}, \qquad \sigma = f_0/[m\bar{\omega}^2(\omega_j^2-\Omega^2)],$$

and where Ω has been introduced to be the response frequency. Using equations (11) as the form of the solution to equations (5), assuming that the linear modal frequencies satisfy $\omega_{jc}^2 \approx \omega_{js}^2 \approx \Omega^2/9$, and proceeding in the usual manner for the method of averaging [3], one finally obtains the following averaged equations:

$$\begin{aligned}
B_j' &= \epsilon\{p(B_jC_j^2\sin(\beta_j-\gamma_j) + \sigma(3B_j^2\sin 3\beta_j + C_j^2\sin(2\gamma_j+\beta_j))) - dB_j\},\\
B_j\beta_j' &= \epsilon B_j\{3pB_j^2 + [2+\cos 2(\beta_j-\gamma_j)]pC_j^2 - \lambda_{jc}\} + \epsilon\sigma p\{3B_j^2\cos 3\beta_j + 2\sigma B_j\\
&\quad + C_j^2\cos(2\gamma_j+\beta_j)\},\\
C_j' &= \epsilon\{p(B_j^2C_j\sin 2(\gamma_j-\beta_j) + 2\sigma B_jC_j\sin(2\gamma_j+\beta_j)) - dC_j\},\\
C_j\gamma_j' &= \epsilon C_j\{[2+\cos 2(\gamma_j-\beta_j)]pB_j^2 + 3pC_j^2 - \lambda_{js}\} +\\
&\quad \epsilon p\sigma\{2B_jC_j\cos(2\gamma_j+\beta_j) + 2\sigma C_j\},
\end{aligned} \quad (12)$$

where

$$\epsilon\bar{\lambda}_{jc} = \omega_{jc}^2 - \frac{\Omega^2}{9}, \qquad \epsilon\bar{\lambda}_{js} = \omega_{js}^2 - \frac{\Omega^2}{9}, \qquad p = \frac{3}{2m\bar{\omega}^2\Omega n^2}\left\{k_2L + \frac{T_2M}{a^4}\right\},$$

$$L = \sum_{i=1}^{n}(\cos i\alpha_j - \cos(i+1)\alpha_j)^4, \qquad M = \sum_{i=1}^{n}\sin^4 i\alpha_j = \sum_{i=1}^{n}\cos^4 i\alpha_j, \qquad d = \frac{3d}{2m\bar{\omega}^2},$$

$$\lambda_{jc} = 3\bar{\lambda}_{jc}/2\Omega, \qquad \lambda_{js} = 3\bar{\lambda}_{js}/2\Omega. \quad (13)$$

In the derivation of equations (12), the following trigonometric identities have been used:

$$\sum_{i=1}^{n}[\cos i\alpha_j - \cos(i+1)\alpha_j]^3[\sin i\alpha_j - \sin(i+1)\alpha_j] = 0,$$

$$\sum_{i=1}^{n} [\cos i\alpha_j - \cos (i+1)\alpha_j][\sin i\alpha_j - \sin (i+1)\alpha_j]^3 = 0,$$

$$\sum_{i=1}^{n} \cos (2i\alpha_j) = 0, \qquad \sum_{i=1}^{n} \sin (2i\alpha_j) = 0. \tag{14}$$

Equations (12) described the subharmonic responses of the nearly cyclic system and their detailed analysis is carried out in the next section.

3. ANALYSIS OF THE CONSTANT SOLUTIONS

The averaged equations for the third order subharmonic response of the cyclic system, equations (12), can be written in the following form:

$$B' = \{BC^2 \sin 2(\beta - \gamma) + \sigma(3B^2 \sin 3\beta + C^2 \sin (2\gamma + \beta)) - dB\},$$

$$B\beta' = B\{3B^2 + [2 + \cos 2(\beta - \gamma)]C^2 - \lambda_c\} + \sigma\{3B^2 \cos 3\beta + 2\sigma B + C^2 \cos (2\gamma + \beta)\},$$

$$C' = \{B^2 C \sin 2(\gamma - \beta) + 2\sigma BC \sin (2\gamma + \beta) - dC\},$$

$$C\gamma' = C\{[2 + \cos 2(\gamma - \beta)]B^2 + 3C^2 - \lambda_s\} + \sigma\{2BC \cos (2\gamma + \beta) + 2\sigma C\}. \tag{15}$$

Since equations (12) are valid for all the degenerate pairs of modes with identical or nearly identical natural frequencies, ω_j, all the subscripts j have been dropped. Also, the non-linear coefficient p has been absorbed in the equations by the change of parameters $\lambda_c/p \to \lambda_c$, $\lambda_s/p \to \lambda_s$, $d/p \to d$, and the time scale change $\tau p \to \tau$. In equations (15), a prime now denotes derivative with respect to the slow time $\epsilon\tau$. Note that the averaged equations, and hence the subharmonic response, depend on the external parameters of the amplitude of excitation in the "cos $-j$" mode, σ, and the two external frequency mistunings λ_s and λ_c. The other important parameter is the system damping constant d. The non-linearity coefficient p influences all the parameters, although only indirectly.

The averaged equations (15) can be written in Cartesian form by using the change of co-ordinates $x_1 = B \cos \beta$, $y_1 = B \sin \beta$, $x_2 = C \cos \gamma$, and $y_2 = C \sin \gamma$. The resulting equations are

$$x_1' = -dx_1 + \lambda_c y_1 - 3y_1 E - 2x_2 M + 2\sigma(3x_1 y_1 + x_2 y_2 - \sigma y_1),$$

$$y_1' = -dy_1 - \lambda_c x_1 + 3x_1 E - 2y_2 M + \sigma(3(x_1^2 - y_1^2) + x_2^2 - y_2^2 + 2\sigma x_1),$$

$$x_2' = -dx_2 + \lambda_s y_2 - 3y_2 E + 2x_1 M + 2\sigma(x_1 y_2 + y_1 x_2 - \sigma y_2),$$

$$y_2' = -dy_2 - \lambda_s x_2 + 3x_2 E + 2y_1 M + 2\sigma(x_1 x_2 - y_1 y_2 + \sigma x_2), \tag{16}$$

where $E = (x_1^2 + y_1^2 + x_2^2 + y_2^2)$ and $M = (x_1 y_2 - y_1 x_2)$.

Equations (16) (or (15)) have three types of steady state constant solutions: the zero subharmonic solution which corresponds to the harmonic response of the system, the single-mode solutions with $C = 0$, and the coupled-mode solutions. These solutions and their stability are considered separately. First note that the zero subharmonic solution ($B = 0, C = 0$) exists for all values of the parameters. One now considers non zero solutions of these equations.

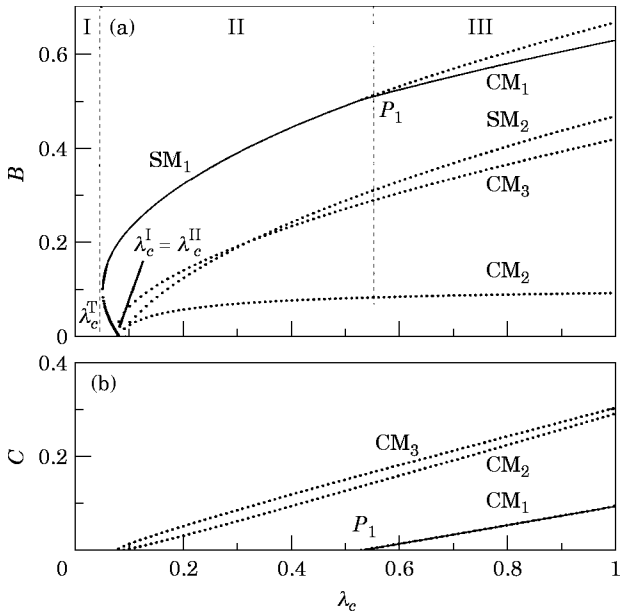

Figure 2. Steady state subharmonic response amplitudes as a function of the excitation frequency λ_c; $d = 0$, $\sigma = 0{\cdot}2$, $\mu = 0$; (a) B, (b) C.

3.1. SINGLE-MODE SOLUTIONS ($x_2 = y_2 = 0$)

Single-mode subharmonic solutions of the undamped system, equations (15) with $d = 0$, are determined by the following equations:

$$3B^2\sigma \sin 3\beta = 0, \qquad 3B^2 + 3\sigma B \cos 3\beta + 2\sigma^2 - \lambda_c = 0. \tag{17}$$

The first of these equations shows that for $B \neq 0$, $\sin 3\beta = 0$ and hence $\cos 3\beta = \pm 1$. Let $\delta \equiv \cos 3\beta = \pm 1$. Then, one notes that there are three single-mode solutions with the same amplitude B, and phase angles defined by $3\beta + 2n\pi$, or $\beta + 2n\pi/3$, where n takes integer values. Thus, these solutions are phase-shifted by $2\pi/3$.

When $\delta = 1$, the amplitude B of single-mode solutions satisfies

$$B = -\sigma/2 + \tfrac{1}{6}\sqrt{3(4\lambda_c - 5\sigma^2)}. \tag{18}$$

The solution branch with $\delta = 1$ is single-valued and it exists only for $\lambda_c \geqslant 2\sigma^2$. It has a zero amplitude when $\lambda_c = 2\sigma^2$. In the next section one will show that it touches the zero subharmonic solution at that point. When $\sigma = -1$, the amplitude B of single-mode solutions satisfies

$$B = \sigma/2 \pm \tfrac{1}{6}\sqrt{3(4\lambda_c - 5\sigma^2)}. \tag{19}$$

The solution branch with $\delta = -1$ has a double root (turning point) when $\lambda_c = 5\sigma^2/4$ and $B = \sigma/2$, it exists for $\lambda_c \geqslant 5\sigma^2/4$, and the smaller of the two solutions becomes zero at $\lambda_c^I = \lambda_c = 2\sigma^2$, where it also touches the zero subharmonic solution (see Figure 2). Thus, for $\lambda_c \geqslant 5\sigma^2/4$, two single-mode subharmonic solutions exist. Furthermore, the lower branch goes to zero at $\lambda_c = 2\sigma^2$ where it forms a cusp point with the branch corresponding to $\delta = 1$. It is clear then that, even in the absence of damping, a minimum of external mistuning is required before the system can exhibit a subharmonic solution in the excited mode.

When damping is present, the phase angle β can be eliminated, and the amplitude of the single-mode solutions can be shown to satisfy the following polynomial in B:

$$9B^4 - 3(2\lambda_c - \sigma^2)B^2 + (\lambda_c - 2\sigma^2)^2 + d^2 = 0. \tag{20}$$

Equation (20) has two roots given by

$$B^2 = (2\lambda_c - \sigma^2 \pm \sqrt{3\sigma^2(4\lambda_c - 5\sigma^2) - 4d^2})/6. \tag{21}$$

For real subharmonic solutions to exist, the mistuning λ_c must satisfy the condition

$$\lambda_c \geqslant d^2/3\sigma^2 + 5\sigma^2/4. \tag{22}$$

For fixed values of σ and d, the turning point in the (λ_c, B) plane occurs when the equality is satisfied in the above relation, and the amplitude of the single-mode response at that point is given by

$$B^2 = (2\lambda_c - \sigma^2)/6. \tag{23}$$

For system parameters satisfying the condition in equation (22), one can verify that both roots of equation (21) are positive. Thus, there always exist two single-mode subharmonic solutions for any value of damping. As noted above, in the absence of damping, the lower branch of single-mode solutions touches the zero subharmonic solution. In the presence of damping, however, the subharmonic solutions lift off away from the trivial solution.

3.2. COUPLED-MODE SOLUTIONS

The equations determining the coupled-mode subharmonic solutions ($B \neq 0$, $C \neq 0$) of the undamped system can be easily obtained from equations (15). For every coupled-mode solution with some phase angle γ, it is easy to see that there is another solution with phase angle $\gamma + \pi$ for the same amplitude C. These equations can be manipulated to obtain the following equations in the amplitudes B and C of the coupled-mode solutions:

$$4(1 - \epsilon_1)B^3 + 3\sigma(3\delta - (2 + \epsilon_1)\epsilon_2)B^2 + (\epsilon_1(\lambda_s - 2\sigma^2) - \lambda_c)B + \epsilon_2\sigma(\lambda_s - 2\sigma^2) = 0, \tag{24}$$

$$C^2 = [\lambda_s - (2 + \epsilon_1)B^2 - 2B\sigma\epsilon_2 - 2\sigma^2]/3 \tag{25}$$

Here, $\delta = \cos 3\beta = \pm 1$, $\epsilon_1 = \cos 2(\beta - \gamma) = \pm 1$ and $\epsilon_2 = \cos(2\gamma + \beta) = \pm 1$. Furthermore, $3\beta = n\pi$, $2(\beta - \gamma) = m\pi$, and $\beta + 2\gamma = (n - m)\pi$, where m and n are integers. Equation (25) shows that the subharmonic amplitude C of the indirectly excited mode has a zero amplitude when

$$\lambda_s - (2 + \epsilon_1)B^2 - 2B\sigma\epsilon_2 - 2\sigma^2 = 0. \tag{26}$$

This should correspond to the condition where the coupled-mode subharmonic solutions may bifurcate from a single-mode subharmonic solution. Stability analysis will allow us to confirm this possibility.

As the above discussion shows, many branches of coupled-mode subharmonic solutions are possible depending on the values assumed by ϵ_1, ϵ_2, and δ and these cases are considered separately.

When $\epsilon_1 = -1$, m is odd, and δ and ϵ_2 take opposite values. When $\delta = -1$ and $\epsilon_2 = 1$, the coupled-mode solutions of equations (24), (25) satisfy

$$8B^3 - 12\sigma B^2 + (2(\sigma^2 - \lambda_c) + \mu)B + \sigma(\lambda_c - \mu - 2\sigma^2) = 0,$$

$$C^2 = \tfrac{1}{3}(\lambda_c - \mu - B^2 - 2B\sigma - 2\sigma^2), \tag{27}$$

where $\mu = \lambda_c - \lambda_s$ is a measure of the internal mistuning. These solutions have two branches which are denoted as CM_1 and CM_2 (Figure 2). The mode component C has a zero amplitude when

$$B^2 + 2B\sigma + 2\sigma^2 - \lambda_c + \mu = 0. \tag{28}$$

By solving equation (28) simultaneously with equation (19), one can find the amplitude B,

$$B = \tfrac{1}{4}(5\sigma \pm \sqrt{25\sigma^2 + 8\mu}), \tag{29}$$

where the coupled-mode solutions meet the single-mode solutions. The corresponding value of mistuning λ_c is

$$\lambda_c = 11\sigma^2/8 + \mu/2 \pm (\sigma/8)\sqrt{25\sigma^2 + 8\mu}. \tag{30}$$

In the case of $\mu \geqslant 0$, there is only one such point at which a coupled-mode solutions branch meets the single-mode solutions. When $0 > \mu \geqslant -25\sigma^2/8$, both branches of the coupled-mode solutions meet single-mode solutions. When $\mu < -25\sigma^2/8$, there are no such points.

When $\delta = 1$ and $\epsilon_2 = -1$, the coupled-mode solution has only one branch which is denoted as CM_3 (Figure 2). Along this branch, the component C has a zero amplitude when

$$B^2 - 2B\sigma + 2\sigma^2 - \lambda_c + \mu = 0. \tag{31}$$

By solving equation (31) simultaneously with equation (19), one finds the values of the amplitude B,

$$B = \tfrac{1}{4}(-5\sigma \pm \sqrt{25\sigma^2 + 8\mu}), \tag{32}$$

where the coupled-mode solutions meet the single-mode solutions. When $\mu > 0$, there is only one such point. There are no such points when $\mu < 0$.

When $\epsilon_1 = 1$ (m is even), δ and ϵ_2 assume the same values (either $+1$ or -1), and the coupled-mode solutions are determined by the following equations:

$$B = \epsilon_2\sigma(\lambda_c - \mu - 2\sigma^2)/(2\sigma^2 + \mu), \qquad C^2 = \tfrac{1}{3}(\lambda_c - \mu - 3B^2 - 2\epsilon_2\sigma B - 2\sigma^2). \tag{33}$$

Clearly, this solution branch is unique and, interestingly, the amplitude B varies linearly with the excitation frequency λ_c. As before, the component C has a zero amplitude when

$$3B^2 + 2\epsilon_2\sigma B + 2\sigma^2 - \lambda_c + \mu = 0. \tag{34}$$

Furthermore, these coupled-mode solutions meet the zero subharmonic solution when $\lambda_c^{II} = 2\sigma^2 + \mu$. By solving equation (34) simultaneously with equations (18), one can show that this branch of the coupled-mode solutions meets the single-mode solutions when

$$B = \mu/\sigma(3\delta - 2\epsilon_2). \tag{35}$$

At this point, the parameters satisfy the relation

$$\lambda_c = \mu(2\sigma^2 + 3\mu)/\epsilon_2\sigma^2(3\delta - 2\epsilon_2) + \mu + \sigma^2. \tag{36}$$

The above analysis shows that, in the absence of damping, single-mode solutions and some of the coupled-mode solutions may meet the zero subharmonic solution. When damping is present, it is difficult to obtain analytical expressions for the amplitudes of steady state coupled-mode solutions. Hence, the effects of damping on the coupled-mode solutions are investigated by using numerical techniques and the results are included in section 5.

4. STABILITY ANALYSIS OF CONSTANT SOLUTIONS

4.1. TRIVIAL SOLUTION

First, the stability of the harmonic response is considered. The eigenvalues of the Jacobian matrix of equations (16) determine the stability properties of the solution at which the Jacobian is evaluated. As it turns out, it is a general feature of the trivial and single-mode solutions that the Jacobian is composed of two 2×2 non-zero blocks along the diagonal. These blocks correspond to disturbances in the subharmonics associated with "cos $-j$" and "sin $-j$" modes, respectively. Then, the eigenvalues which determine the stability of the zero subharmonic solution can be shown to satisfy the following characteristic equations:

$$\Lambda^2 + 2d\Lambda + d^2 + (\lambda_c - 2\sigma^2)^2 = 0, \qquad \Lambda^2 + 2d\Lambda + d^2 + (\lambda_c - \mu - 2\sigma^2)^2 = 0. \tag{37}$$

For each pair of eigenvalues with $d > 0$, it is easy to see that all eigenvalues are complex with negative real parts. Thus, the zero subharmonic solution is always stable. Even in the absence of damping, the zero subharmonic solution is stable everywhere except at the isolated points $\lambda_c^{\mathrm{I}} = 2\sigma^2$ and $\lambda_c^{\mathrm{II}} = \mu + 2\sigma^2$, where there are two zero eigenvalues. At the parameter point $\lambda_c^{\mathrm{I}} = 2\sigma^2$, it was shown in the previous section that the two single-mode subharmonic solutions meet in a cusp point and touch the zero solution. Again, when $\lambda_c^{\mathrm{II}} = 2\sigma^2 + \mu$, the coupled-mode solutions corresponding to $\epsilon_1 = 1$ meet at the zero subharmonic solution.

4.2. SINGLE-MODE SOLUTIONS

There are three sets of single-mode solutions which are phase-shifted by $2\pi/3$. When $d = 0$, each single-mode solution set has two branches, one with $\delta = 1$ and the other with $\delta = -1$. For solutions with $\delta = -1$ or $+1$, the eigenvalues corresponding to the single-mode solutions satisfy

$$\Lambda^2 + (\lambda_c - 3B^2 \mp 6\sigma B - 2\sigma^2)(\lambda_c - 9B^2 \pm 6\sigma B - 2\sigma^2) = 0, \tag{38}$$

$$\Lambda^2 + (\lambda_c - \mu - B^2 \mp 2\sigma B - 2\sigma^2)(\lambda_c - \mu - 3B^2 \pm 2\sigma B - 2\sigma^2) = 0, \tag{39}$$

where the two signs are for $\delta = -1$ and $+1$, respectively.

For $\delta = -1$, one of the eigenvalues, a root of equation (38), is zero when $x_1 = -B = -\sigma/2$ and $\lambda_c = 5\sigma^2/4$, which is also the condition for the existence of a turning point. When $B = 0$, there are two zero eigenvalues each at the isolated parameter points $\lambda_c = 2\sigma^2$ and $\lambda_c = 2\sigma^2 + \mu$, where the single-mode solutions touch the zero subharmonic solution and the coupled-mode solutions touch the zero subharmonic solution.

In the previous section, one has seen that, when $\epsilon_1 = -1$, $\epsilon_2 = 1$, and $\delta = -1$, equation (28) gives the conditions where the coupled-mode solutions branch touches the single-mode solutions branch. Equation (39) confirms that the single-mode solution with $\delta = -1$ has a zero eigenvalue at the corresponding point, and hence, it is a pitchfork bifurcation point. Depending on the value of μ, we have seen that there may be two, one, or zero pitchfork bifurcation points. Similarly, the single-mode solution has a zero eigenvalue when $\epsilon_1 = 1$, $\epsilon_2 = -1$, and $\delta = -1$, and $\lambda_c - \mu - 3B^2 + 2\sigma B - 2\sigma^2 = 0$. This is, thus, another pitchfork bifurcation point and the corresponding coupled-mode solution bifurcates from the single-mode solution, as shown in equation (34).

It was shown earlier that the coupled-mode solution with $\epsilon_1 = \epsilon_2 = -1$ and $\delta = 1$ touches the single-mode solution when it satisfies $\lambda_c - \mu - B^2 + 2\sigma B - 2\sigma^2 = 0$ for $\mu > 0$ (equation (31)). Equation (39) confirms that the single-mode solution has a zero eigenvalue at the corresponding point and, hence, it is a pitchfork bifurcation point. Similarly, the single-mode solution has another zero eigenvlaue when $\epsilon_1 = \epsilon_2 = 1$, $\delta = 1$, $\mu > 0$, and

$\lambda_c - \mu - 3B^2 - 2\sigma B - 2\sigma^2 = 0$. This is another pitchfork bifurcation point and the corresponding coupled-mode solution bifurcates from the single-mode solution (equation (34)).

In the presence of damping, a stability analysis of the single-mode solutions, and the stability of coupled-mode subharmonic solutions, is algebraically very tedious. One, thus, now turns to numerical bifurcation analysis of the averaged equations (16). The results of this analysis, along with those from direct numerical simulation of the averaged equations, are given in the next section.

5. NUMERICAL RESULTS

The averaged equations (15) depend on four parameters: d, λ_c, λ_s and σ. Numerical results are presented here in the form of amplitude–frequency response curves and in terms of bifurcation sets. For most results, the excitation amplitude is held constant at $\sigma = 0{\cdot}2$.

Figure 2 shows the zero subharmonic solution, and the various single-mode and coupled-mode constant solutions B and C, for zero damping ($d = 0$) and zero internal mistuning ($\mu = 0$), as a function of the frequency mistuning λ_c. The frequency axis is divided into three intervals I, II and III, according to the nature of solutions. Over the interval I, only the stable zero subharmonic solution exists. Over the interval II, a stable single-mode solution coexists with the stable zero subharmonic solution and other unstable single-mode and coupled-mode subharmonic solutions. Over the interval III, a stable coupled-mode solution coexists with the stable zero subharmonic solution and other unstable solutions. In this figure, SM_1 represents the single-mode solution branch with $\delta = -1$. It has a turning point at $\lambda_c^T = 5\sigma^2/4$, where it undergoes a saddle-node bifurcation. At P_1, this single-mode branch undergoes a supercritical pitchfork bifurcation, giving rise to the stable coupled-mode solutions branch CM_1. The symbols CM_1 and CM_2 represent the coupled-mode subharmonic branches with $\epsilon_1 = -1$, $\delta = -1$, and $\epsilon_2 = 1$. The single-mode subharmonic branch with $\delta = 1$, denoted as SM_2, is single-valued and unstable. The symbol CM_3 represents the coupled-mode solutions branch with $\epsilon_1 = \epsilon_2 = -1$ and $\delta = 1$. The solution branches SM_1 and SM_2, and the solution branches CM_2 and CM_3, meet the zero subharmonic solution at the isolated parameter point $\lambda_c^I = \lambda_c^{II} = 2\sigma^2$. Note that, for every single-mode solution with some phase angle β, there are two other single-mode solutions which are phase-shifted by $2\pi/3$ and $4\pi/3$ for the same amplitude B. Also, for every coupled-mode solution with some phase angle γ, there is another coupled-mode solution with phase angle $\gamma + \pi$ for the same amplitude C. In Figure 2, and in later figures, stable solutions are denoted by solid curves and the unstable solutions are denoted by dotted curves.

Figures 3 and 4 show the effect of internal mistuning on the subharmonic response of the undamped system. Figure 3 represents the response curves for $\mu = 0{\cdot}1$. When the internal mistuning, μ, increases, the pitchfork point P_1 moves to the right along the single-mode solutions branch SM_1. Hence, it increases the extent of the interval II, where the stable single-mode solution coexists with the zero subharmonic solution which is now stable everywhere except at the isolated points λ_c^I and λ_c^{II} (P_0). The single-mode solutions branch SM_2 undergoes pitchfork bifurcations at the points P_2 and P_4. At P_2, the coupled-mode solution branch CM_3 bifurcates from the single-mode solution branch SM_2. At P_4, the coupled-mode solutions branch CM_4 with $\epsilon_1 = \epsilon_2 = \delta = 1$ terminates at the single-mode solutions branch SM_2. The coupled-mode solutions branches CM_4 and CM_2 meet the zero subharmonic solution at P_0.

Figure 4 represents the response curves for $\mu = -0{\cdot}1$. As seen in the analysis, when mistuning satisfies the condition $0 > \mu \geqslant -25\sigma^2/8$, the single-mode solutions branch SM_1

has two pitchfork bifurcation points, P_1 and P_3. As $\mu \to -25\sigma^2/8$, these two pitchfork points get closer, and they merge at the parameter point $\lambda_c = 47\sigma^2/16$. When $\mu < 0$, the coupled-mode branch CM_4 bifurcates from the single-mode solutions branch SM_1, and the coupled-mode solution branches CM_3 and CM_4 meet the zero subharmonic solution at the isolated parameter point P_0.

Figure 5 represents the pitchfork bifurcation set in the (λ_c, μ) plane for the coupled-mode solutions at a fixed forcing amplitude $\sigma = 0{\cdot}2$ and $d = 0$. Obviously, it corresponds to bifurcations from the single-mode solutions to coupled-mode solutions at a zero eigenvalue. When $\mu > 0$, there are three pitchfork points, P_1, P_2 and P_4. When $0 > \mu \geqslant -25\sigma^2/8$, the pitchfork points P_1, P_3, and P_4 exist, and for $\mu < -25\sigma^2/8$, only the pitchfork point P_4 exists. As $\mu \to 0$, all but P_1 converge to the isolated point λ_c^{I}.

Next, we investigate the qualitative changes in response curves that take place as the damping is introduced. Figure 6 represents a set of response curves for $\sigma = 0{\cdot}2$ and $\mu = 0$. These were obtained using AUTO [11], and are given in terms of Cartesian amplitude components. As shown in the analysis, in the presence of damping, single-mode and coupled-mode solutions do not meet the zero subharmonic solution. In Figure 6, λ_{SNS} represents a saddle-node bifurcation point on the single-mode solutions branch. Also, whereas λ_{HB} represents a Hopf bifurcation point, λ_{SNC_1} and λ_{SNC_2} represent saddle-node bifurcation points on the coupled-mode solutions. Figure 6(a) is for $d = 0{\cdot}1$. When $\lambda_{SNS} \leqslant \lambda_c \leqslant \lambda_{SNC_1}$ and $\lambda_{SNC_1} \leqslant \lambda_c \leqslant \lambda_{PF_1}$, three stable branches of single-mode subharmonic solutions coexist with the stable zero subharmonic solution. These three solutions are just the phase-shifted copies of the same solution and have the same amplitude $(B = \sqrt{x_1^2 + x_2^2})$. When $\lambda_c \geqslant \lambda_{PF_1}$, only the zero subharmonic solution is stable. Figure 6(b) is for $d = 0{\cdot}01$ When $\lambda_{SNS} \leqslant \lambda_c \leqslant \lambda_{PF_1}$, three stable branches of single-mode constant solutions coexist with the stable zero subharmonic solution. When $\lambda_{PF_1} \leqslant \lambda_c \leqslant \lambda_{SNC_2}$, three

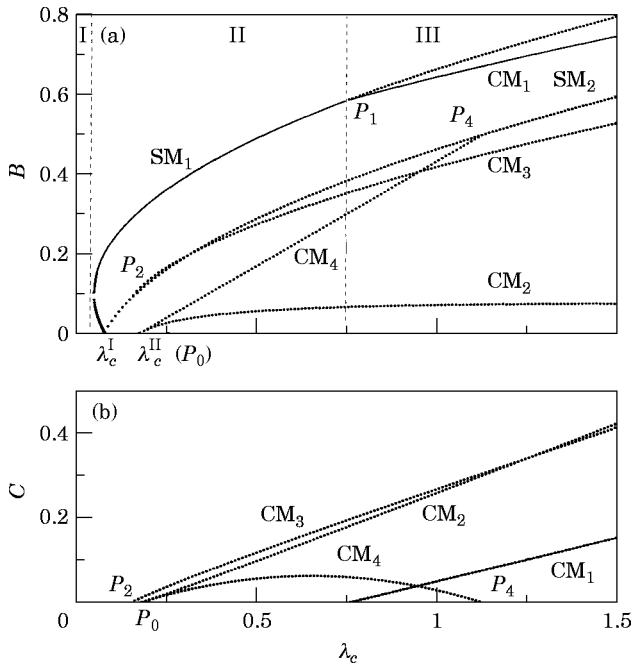

Figure 3. Steady state subharmonic response amplitudes as a function of the excitation frequency λ_c; $d = 0$, $\sigma = 0{\cdot}2$, $\mu = 0{\cdot}1$; (a) B, (b) C.

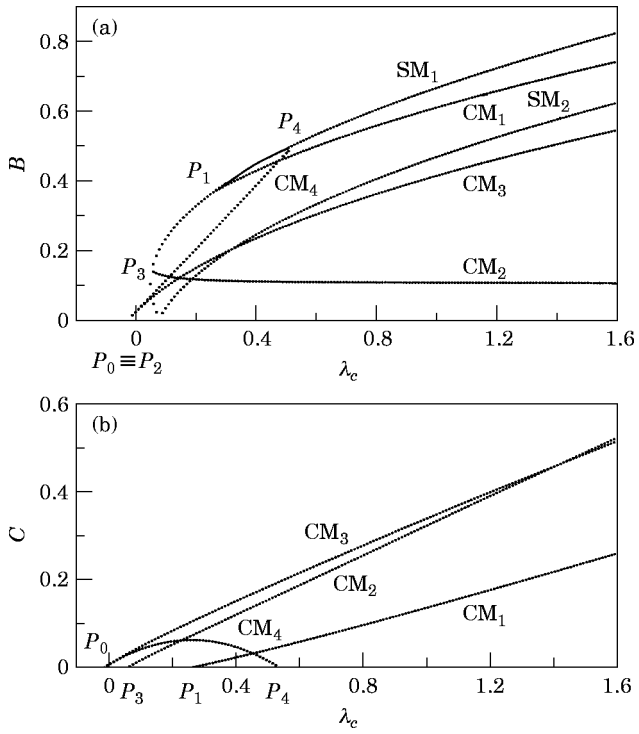

Figure 4. Steady state subharmonic response amplitudes as a function of the excitation frequency λ_c; $d = 0$, $\sigma = 0{\cdot}2$, $\mu = -0{\cdot}1$; (a) B, (b) C.

stable branches of coupled-mode solutions coexist with the stable zero subharmonic solution. For the given parameter values, when $\lambda_c > \lambda_{SNC_2}$, the only stable constant solution is the zero subharmonic solution.

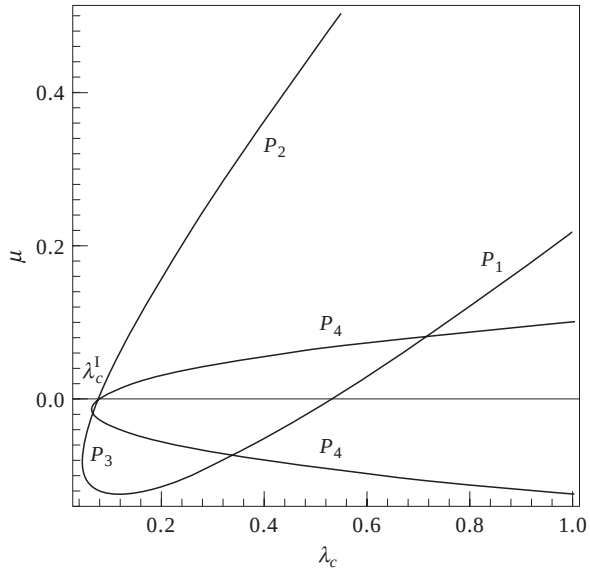

Figure 5. Pitchfork bifurcation sets for the steady state constant solutions in the (λ_c, μ) plane; $\sigma = 0{\cdot}2$, $d = 0{\cdot}0$.

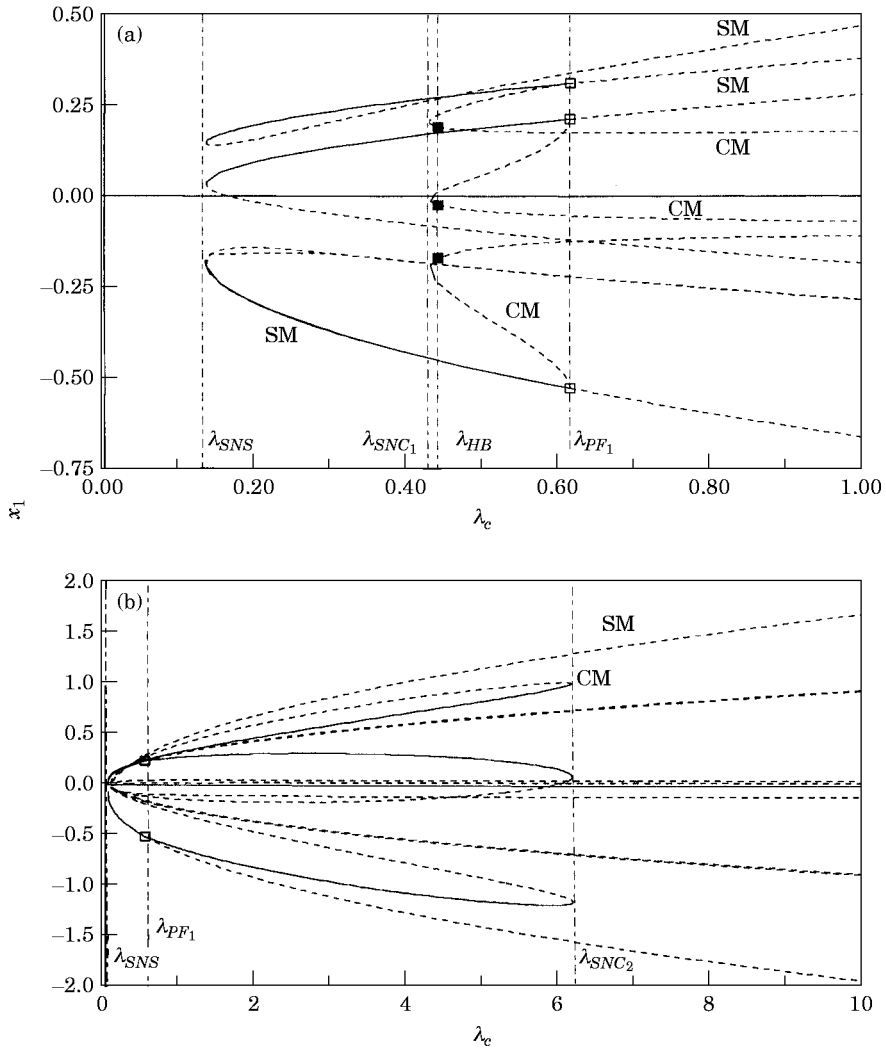

Figure 6. Steady state subharmonic response amplitudes as a function of the excitation frequency λ_c; $\sigma = 0{\cdot}2$, $\mu = 0$; (a) $d = 0{\cdot}1$, (b) $d = 0{\cdot}01$.

Figure 7 represents bifurcation sets in the (λ_c, d) plane for the coupled-mode solutions, in the absence of internal mistuning. When $d < 0{\cdot}05$, the coupled-mode solution has two saddle-node bifurcation points, λ_{SNC_1} and λ_{SNC_2}. As $d \to 0$, one of the saddle-node bifurcation points (λ_{SNC_2}) becomes unbounded and occurs at ∞. As $d \to 0{\cdot}05$, the saddle-node point λ_{SNC_2} approaches the pitchfork point λ_{PF_1} (compare Figures 6(a) and 6(b)). When $0{\cdot}05 < d < 0{\cdot}53$, there is only one saddle-node point (λ_{SNC_1}) on the coupled-mode solutions branch and there is a Hopf bifurcation point (λ_{HB}) close to the λ_{SNC_1}. The corresponding coupled-mode solution is found to be unstable everywhere except between λ_{SNC_1} and λ_{HB}. As $d \to 0{\cdot}53$, the saddle-node point λ_{SNC_1} approaches the pitchfork point λ_{PF_1}. When $d > 0{\cdot}53$, the coupled-mode solution has no saddle-node points and it is stable between λ_{PF_1} and λ_{HB}. Therefore, damping determines the length of the interval where stable coupled-mode solutions coexist with the stable zero subharmonic solution. In contrast to the primary resonance case, damping does not suppress any branch of

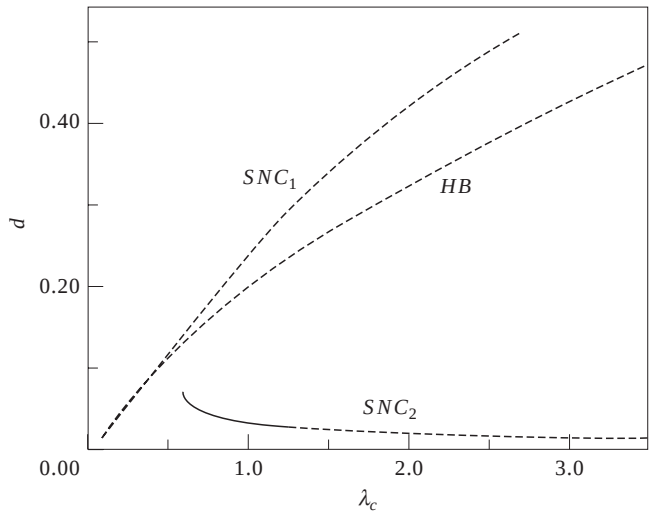

Figure 7. Bifurcation sets for the coupled-mode subharmonic solutions; $\sigma = 0{\cdot}2$, $\mu = 0$.

single-mode or coupled-mode solutions. Damping shifts the solutions to higher frequencies. This phenomonen is also observed in subharmonic solutions of single-degree-of-freedom systems [10], as well as other two-degree-of-freedom sytstems [6].

The effect of internal mistuning on subharmonic solutions in the presence of damping is now considered. Figure 8 shows a bifurcation set in the (λ_c, μ) plane for constant solutions at the fixed amplitude of forcing $\sigma = 0{\cdot}2$ and the fixed value of damping $d = 0{\cdot}1$. This bifurcation set corresponds to a pitchfork bifurcation from the single-mode solutions to the coupled-mode solutions at a zero eigenvalue. For $\mu < 0{\cdot}06$ there is only one pitchfork bifurcation point, and for $\mu > 0{\cdot}06$ there are three pitchfork bifurcation points.

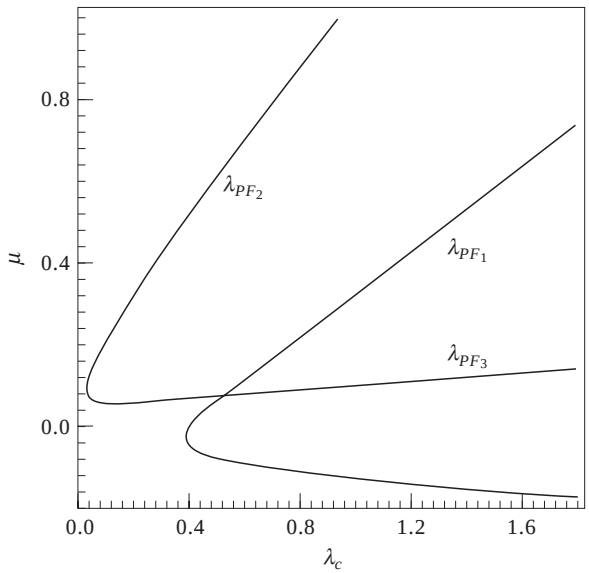

Figure 8. Pitchfork bifurcation sets for the single-mode subharmonic solutions; $\sigma = 0{\cdot}2$, $d = 0{\cdot}1$.

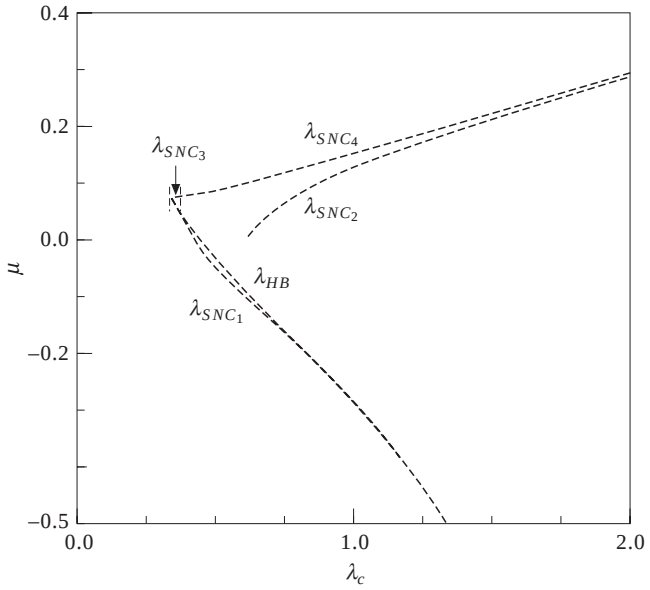

Figure 9. Bifurcation sets for the coupled-mode constant solutions in the (λ_c, μ) plane; $\sigma = 0{\cdot}2$, $d = 0{\cdot}1$.

This bifurcation set was generated via the zero eigenvalue condition for the damped case by using the symbolic algebra software MAPLE.

Figure 9 shows bifurcation sets in (λ_c, μ) plane which correspond to saddle-node and Hopf bifurcations from the coupled-mode solutions branches. These bifurcation sets are for $\sigma = 0{\cdot}2$ and $d = 0{\cdot}1$, and were generated using two-parameter continuation capabilities of the software AUTO. Depending on the value of the internal mistuning μ, there may be as many as four saddle-node bifurcation points. For internal mistuning below $\mu \approx 0{\cdot}003$, the coupled-mode solution has only one saddle-node bifurcation point λ_{SNC_1}. The pitchfork point λ_{PF_1} in Figure 6 is subcritical and the coupled-mode solution is unstable everywhere except over the interval $\lambda_{SNC_1} \leqslant \lambda_c \leqslant \lambda_{HB}$ (Figure 6). When $\mu \approx 0{\cdot}003$, the pitchfork point λ_{PF_1} becomes supercritical and the saddle-node point λ_{SNC_2} arises. The saddle-node point λ_{SNC_2} exists for all values of $\mu > 0{\cdot}003$. When $0{\cdot}06 < \mu < 0{\cdot}0752$, there are three pitchfork points and there are two coupled-mode branches (see Figure 10). One coupled-mode branch is an unstable branch connecting pitchfork points λ_{PF_2} and λ_{PF_3}. As $\mu \to 0{\cdot}0752$, these two coupled-mode branches collide and a separation of branches takes place, thus creating saddle-node bifurcation points λ_{SNC_3} and λ_{SNC_4}. The saddle-node point λ_{SNC_3} exists over a small interval of μ and it joins with λ_{SNC_1}. Saddle-node points λ_{SNC_2} and λ_{SNC_4} exist for all values of $\mu > 0{\cdot}077$.

Periodic solutions of the averaged equations for the level of damping $d = 0{\cdot}1$ are now discussed. The Hopf bifurcation point λ_{HB} (Figure 6) is a supercritical Hopf bifurcation point. Periodic solutions of the averaged equations arise at this Hopf bifurcation point. The periodic solutions in the supercritical periodic branch exhibit period-doubling bifurcation leading to chaotic solutions. This periodic solutions branch, continued by using AUTO, is shown in Figure 11. Here, solid circles represent stable limit cycle solutions, whereas open circles represent unstable solutions. There are two types of changes in the stability, one at turning points in the branch and the other in the interior of the segments between turning points. The latter are where period-doubling bifurcations take place [9]. A representative set of phase-space projections of solutions in the periodic branch is shown

in Figure 12. As $\lambda_c \to 0{\cdot}4532$, the period of the periodic solutions approaches ∞. Consequently, periodic solutions approach a heteroclinic orbit [12] which is asymptotic to a saddle-type coupled-mode constant solution of the averaged equations (Figure 12(d)). When $\lambda_c \approx 0{\cdot}4532$, this heteroclinic orbit collides with the stable manifolds of a single-mode constant solution, and ultimately settles down to a stable single-mode solution (Figure 12(e)).

Let the subharmonic responses for $d = 0{\cdot}1$ and $\mu = 0{\cdot}0$, as already given in Figure 6(a) be recalled. Simulations show that when $0{\cdot}4532 < \lambda_c < 0{\cdot}645$, there are no stable periodic solutions of the averaged system. Also, note that single-mode constant solutions are unstable when $\lambda_c > \lambda_{PF_1}$ and have a complex conjugate pair of eigenvalues with negative real parts, one positive real eigenvalue and a negative real eigenvalue. Furthermore, there are six branches of single-mode constant solutions. At $\lambda_c = 0{\cdot}656$, numerical simulations (see Figure 13) show the formation of a heteroclinic orbit connecting stable and unstable manifolds of three of the single-mode solutions which have the same eigenvalues.

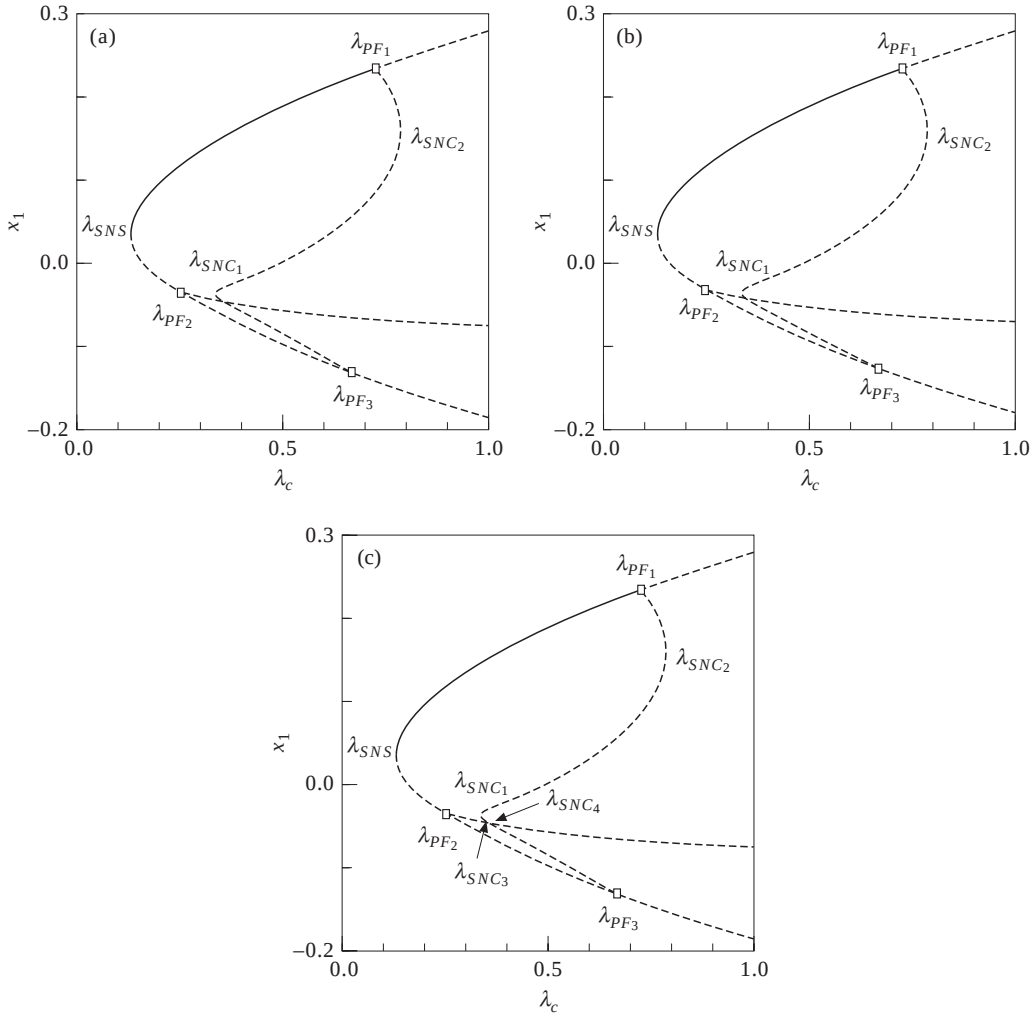

Figure 10. Steady state response amplitudes as a function of the excitation frequency λ_c; $\sigma = 0{\cdot}2$, $d = 0{\cdot}1$; (a) $\mu = 0{\cdot}075$, (b) $\mu = 0{\cdot}0753$, (c) $\mu = 0{\cdot}0755$.

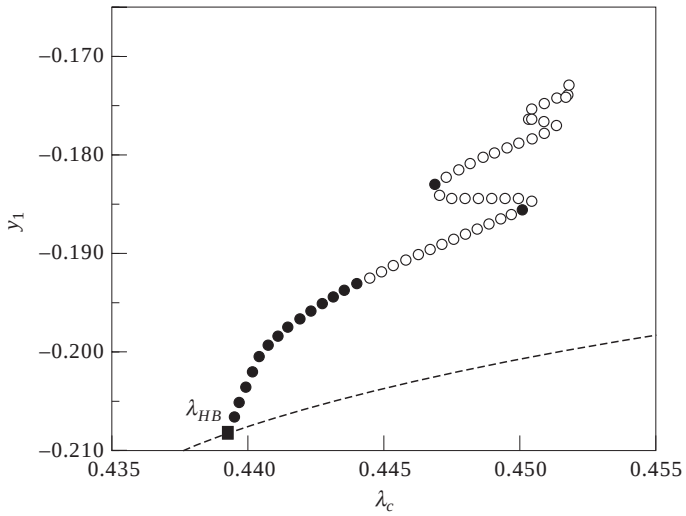

Figure 11. Periodic solutions branch continued from the Hopf bifurcation point on the coupled-mode solution; $\sigma = 0{\cdot}2$, $d = 0{\cdot}1$, $\mu = 0$.

At $\lambda_c = 0{\cdot}6561$, these single-mode constant solutions have eigenvalues $\lambda_{1,2} = -0{\cdot}1 \pm 1{\cdot}14991i$, $\lambda_3 = 0{\cdot}00982473$ and $\lambda_4 = -0{\cdot}209825$. It is easy to shown that now the Sil'nikov conditions [12, 13] for a gluing bifurcation [12] are satisfied. When $\lambda_c < 0{\cdot}656$, two stable periodic orbits appear, and when $\lambda > 0{\cdot}656$ a single periodic orbit is present. Figure 14 shows the numerical evidence of gluing bifurcation for damping $d = 0{\cdot}1$ and zero internal mistuning ($\mu = 0$). The two stable periodic orbits, which appear near the gluing bifurcation point, exist over the interval $0{\cdot}645 < \lambda_c < 0{\cdot}656$. As λ_c decreases to 0·645, these periodic orbits collide with the stable manifold of the saddle-type single-mode subharmonic solutions and ultimately settle down to the zero subharmonic solution.

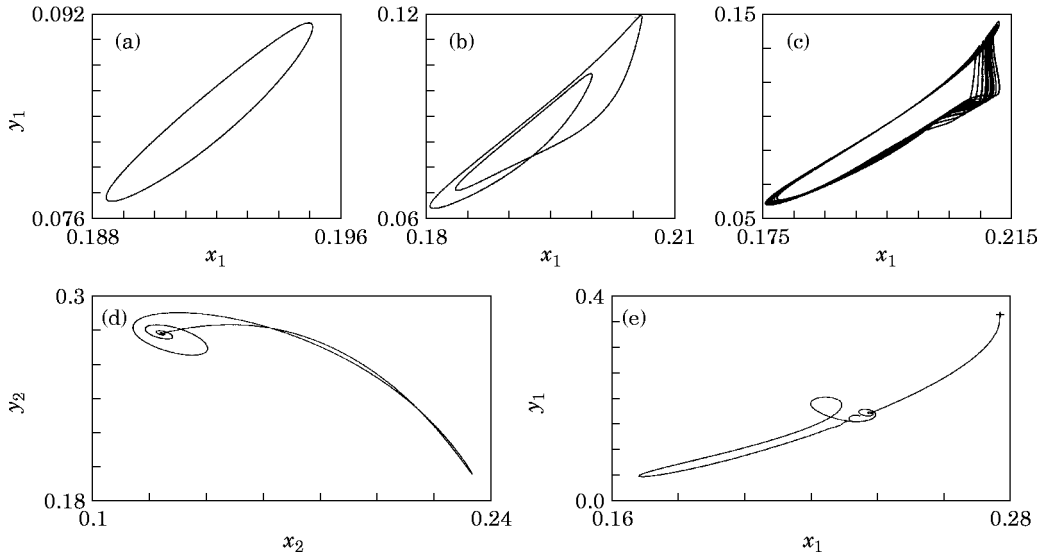

Figure 12. Phase plots for the steady state solutions; $\sigma = 0{\cdot}2$, $d = 0{\cdot}1$, $\mu = 0{\cdot}0$; (a) $\lambda_c = 0{\cdot}44$, (b) $\lambda_c = 0{\cdot}446$, (c) $\lambda_c = 0{\cdot}448$, (d) $\lambda_c = 0{\cdot}453$, (e) $\lambda_c = 0{\cdot}4532$.

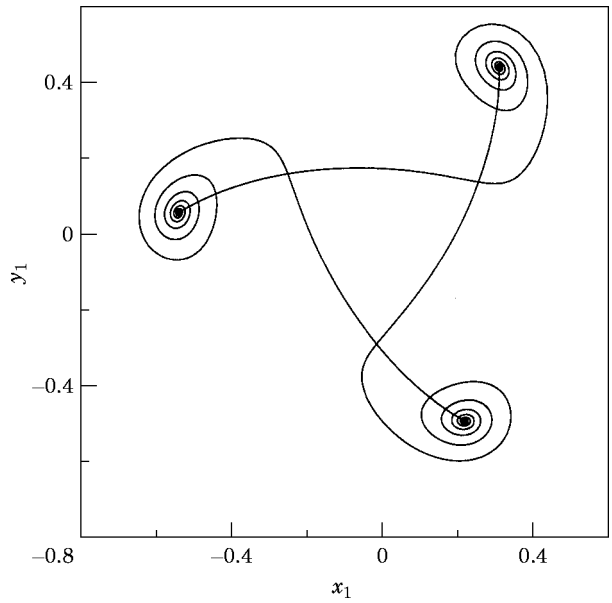

Figure 13. Orbit heteroclinic to steady state single-mode constant solutions; $\lambda_c = 0{\cdot}656$, $d = 0{\cdot}1$, $\mu = 0{\cdot}0$, $\sigma = 0{\cdot}2$.

The single coupled-mode periodic orbit, which appears near the gluing bifurcation point, undergoes a period-doubling bifurcation leading to chaotic motions near $\lambda_c = 0{\cdot}73$, and around $\lambda_c = 4{\cdot}38$, it reverses to a period one solution. The resulting period one solution collides, around $\lambda_c = 4{\cdot}399$, with the stable manifold of the saddle-type single-mode subharmonic solutions and ultimately settles down to the zero subharmonic solution. Thus, a chaotic solution coexists with the stable zero subharmonic solution over the interval $0{\cdot}73 < \lambda_c < 4{\cdot}38$. Figure 15 represents a chaotic motion at $\lambda_c = 3$.

6. TWO-MODE APPROXIMATION OF THE EQUATIONS OF MOTION

When the non-linear response of equations (5) is small, that is, the parameter ϵ is sufficiently small, the solutions of the averaged equations can be used to draw conclusions regarding the behavior of the original system. Constant solutions of the averaged equations correspond to periodic solutions of the non-autonomous equations (5), and periodic solutions of the averaged equations correspond to almost periodic solutions of equations (5). However, these predictions may be valid only for sufficiently small ϵ, and may not be

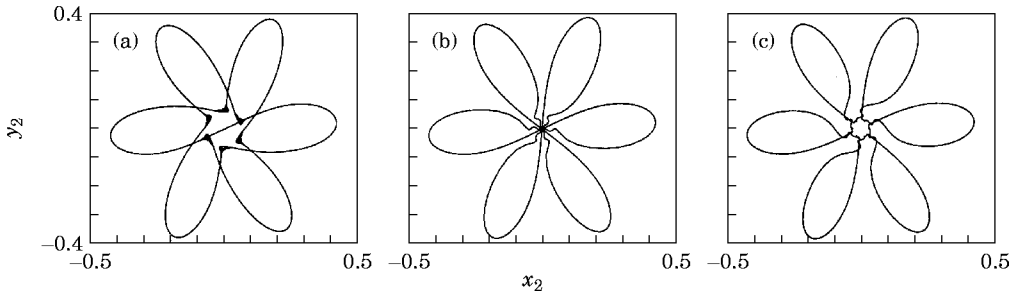

Figure 14. Evidence of gluing bifurcation; $d = 0{\cdot}1$, $\mu = 0{\cdot}0$, $\sigma = 0{\cdot}2$; (a) $\lambda_c = 0{\cdot}65$, (b) $\lambda_c = 0{\cdot}656$, (c) $\lambda_c = 0{\cdot}66$.

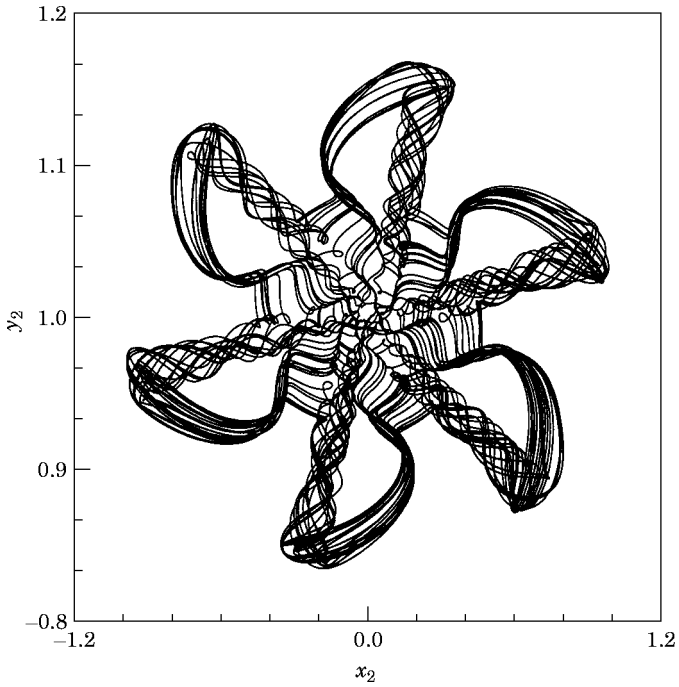

Figure 15. Chaotic solution of the averaged equations; $\lambda_c = 3{\cdot}0$, $d = 0{\cdot}1$, $\mu = 0{\cdot}0$, $\sigma = 0{\cdot}2$.

valid for problems of physical interest. It is also expected that chaotic solutions of the averaged equations correspond to chaotic solutions of equations (5), at least for sufficiently small excitation amplitudes [13]. In order to discuss and quantitatively verify the connection between solutions of the averaged equations and the corresponding solutions of equations (5), one obtains a two-mode approximation of equations (5) where the two modes of interest are the interacting modes in 1:1 internal resonance. These equations apply for all such two-mode pairs with 1:1 resonance.

One assumes that the response of the cyclic structure is given by

$$[\mathbf{X}] = \sum_{j=1}^{n} a_j[\mathbf{V}_j], \tag{40}$$

where $\{\mathbf{V}_1, \mathbf{V}_2 \cdots, \mathbf{V}_n\}$ is an orthogonal set of modes of the linear, undamped system (5) with $\epsilon = 0$, and a_j is the amplitude of the $\mathbf{V}_j$ mode. Substituting the solution form in equation (40) into equations (5), and using the fact that $\mathbf{V}_j$'s are mutually orthogonal, one can derive the following equations for any pair of modes in 1:1 internal resonance:

$$a_k'' + \omega_j^2 a_k = \mathbf{V}_k \cdot (\epsilon \mathbf{F}^{ex} - \mathbf{F}), \qquad a_l'' + \omega_j^2 a_l = \mathbf{V}_l \cdot (\epsilon \mathbf{F}^{ex} - \mathbf{F}). \tag{41}$$

In the subharmonic resonance case, one can derive the following equations for the amplitudes Z_1 and Z_2 of "cos $-$ j" and "sin $-$ j" modes, respectively, when the external excitation is distributed in the form of the "cos $-$ j" mode:

$$\begin{aligned} Z_1'' + \omega_j^2 Z_1 &= -(1/m\bar{\omega}^2)\{\epsilon(AZ_1(Z_1^2 + Z_2^2) + dZ_1') + \mu \cos(\Omega\tau)\}, \\ Z_2'' + \omega_j^2 Z_2 &= -(1/m\bar{\omega}^2)\epsilon(AZ_2(Z_1^2 + Z_2^2) + dZ_2'). \end{aligned} \tag{42}$$

Also, the non-linearity parameter is $A = (1/e^4)\{k_2 L + T_2 M/a^4\}$.

Finally, one considers some solutions for the two-mode approximation of the original equations for parameter values where the subharmonic responses have been predicted using the averaged equations. Figures 16(a–d) represent the response of the approximate equations (42), as obtained by a direct time integration. For the given parameter values, Figures 16(a, b) show a stable coupled-mode subharmonic solution with the coexisting stable harmonic response. The corresponding time responses for Z_1, for the two cases, are given in Figures 16(c–d). Figure 17 represents the Poincaré section of amplitude-modulated subharmonic motion at $\lambda_c = 3{\cdot}0$. For both of these figures, the other parameters were set at $\mu = 0$, $d = 0{\cdot}1$, and $\epsilon = 0{\cdot}1$.

7. SUMMARY

In this work, the third order subharmonic resonance response of the cyclic system with 1:1 internal resonance has been studied. The averaged equations for this case depend on the damping, the forcing amplitude and the internal and external mistunings. A careful bifurcation analysis of the steady state constant solutions of the averaged equations has been performed. Non-trivial subharmonic solutions are shown to be sensitive to variations in damping and internal mistuning. In the undamped case, single-mode solutions and some of the coupled-mode solutions meet the zero subharmonic solution. Damping separates non-trivial subharmonic solutions from the zero subharmonic solution. The analysis of steady state constant solutions and their stability are presented, along with numerical simulations. Periodic solutions are found to exist in these averaged equations and they exhibit period-doubling bifurcation leading to chaotic solutions. The existence of heteroclinic orbits bi-asymptotic to saddle-focus type fixed points and satisfying Sil'nikov-type conditions, and the presence of gluing bifurcation and chaotic dynamics, are observed. The results of a careful direct time integration show a good correspondence

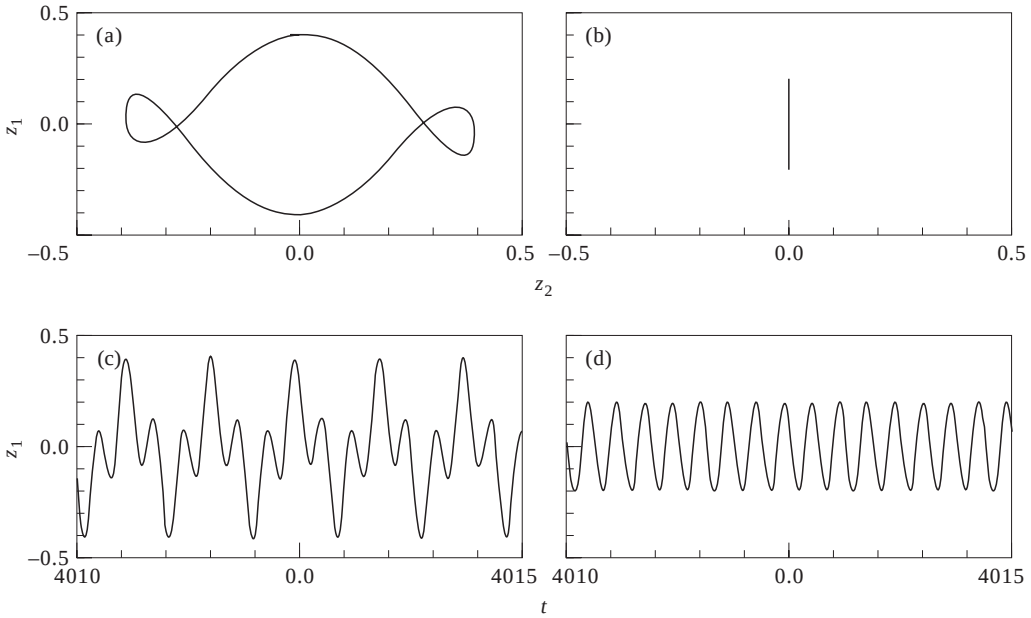

Figure 16. Phase plots for steady state solutions of two-mode approximation of the original system; $\lambda_c = 0{\cdot}6$, $d = 0{\cdot}1$, $\mu = 0{\cdot}0$, $\sigma = 0{\cdot}2$, $\epsilon = 0{\cdot}1$. (a) Coupled-mode subharmonic response; (b) Co-existing harmonic response; (c) corresponding time response for coupled-mode subharmonic response; (d) co-existing harmonic response.

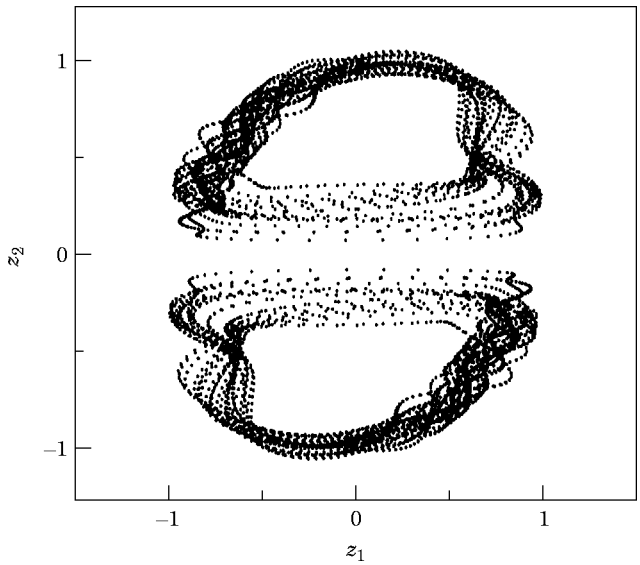

Figure 17. Poincaré section of an amplitude-modulated solution of the two-mode approximation of the original equations; $\lambda_c = 3{\cdot}0$, $d = 0{\cdot}1$, $\mu = 0{\cdot}0$, $\sigma = 0{\cdot}2$, $\epsilon = 0{\cdot}1$.

between the predictions of the averaged system and those of the two-mode approximation of the original system.

REFERENCES

1. G. S. Happawana 1994 *Ph. D. Thesis. Purdue University*, *West Lafayette*, *IN*. Structural analysis of mistuned spatially periodic systems: a singular perturbation approach.
2. A. F. Vakakis 1992 *Acta Mechanica* **95**, 197–226. Dynamics of a non-linear periodic structure with cyclic symmetry.
3. S. Samaranayake, A. K. Bajaj and O. D. I. Nwokah 1995 *Acta Mechanica* **109**, 101–125. Amplitude modulated dynamics and bifurcations in the resonant response of a structure with cyclic symmetry.
4. D. T. Mook, R. H. Plaut and N. Haquang 1985 *Journal of Sound and Vibration* **102**, 473–492. The influence of an internal resonance on non-linear structural vibrations under subharmonic resonance conditions.
5. I. M. K. Shyu, R. H. Plaut and D. T. Mook 1993 *Non-linear Dynamics* **4**, 337–356. Whirling of a forced cantilevered beam with static deflection. II. Superharmonic and subharmonic resonances.
6. A. F. Vakakis 1992 *Non-linear Dynamics* **3**, 123–143. Fundamental and subharmonic resonances in a system with a "1:1" internal resonance.
7. T. A. Nayfeh and A. F. Vakakis 1994 *International Journal of Non-linear Mechanics* **29**, 233–245. Subharmonic traveling waves in a geometrically non-linear circular plate.
8. R. Courant and D. Hilbert 1953 *Methods of Mathematical Physics*. New York: Interscience Publishers.
9. J. Guckenheimer and P. Holmes 1990 *Non-linear Oscillations*, *Dynamical Systems and Bifurcation of Vector Fields*. New York: Springer-Verlag.
10. A. H. Nayfeh and D. T. Mook 1979 *Non-linear Oscillations*. New York: Wiley Interscience.
11. E. Doedel 1986 *AUTO*: *Software for continuation and bifurcation problems in ordinary differential equations*, Department of Applied Mathematics, California Institute of Technology, Pasadena, CA.
12. J. M. Gambaudo, P. Glendinning and C. Tresser 1985 *Journal de Physique Lettres* **46**, 653–657. Stable cycles with complicated structure.
13. A. K. Bajaj and J. M. Johnson 1992 *Philosophical Transactions of the Royal Society of London* **A338**, 1–41. On the amplitude dynamics and 'crisis' in resonant motion of stretched strings.